

# Structure and bonding of dense liquid oxygen from first principles simulations

Burkhard Militzer, François Gygi, and Giulia Galli  
*Lawrence Livermore National Laboratory, Livermore, CA 94550*  
 (Dated: November 9, 2018)

Using first principles simulations we have investigated the structural and bonding properties of dense fluid oxygen up to 180 GPa. We have found that band gap closure occurs in the molecular liquid, with a “slow” transition from a semi-conducting to a poor metallic state occurring over a wide pressure range. At approximately 80 GPa, molecular dissociation is observed in the metallic fluid. Spin fluctuations play a key role in determining the electronic structure of the low pressure fluid, while they are suppressed at high pressure.

The study of pressure-induced transformations in solids and liquids has become an active field of research in the last decade [1], due to key progress both in experimental methods (diamond anvil cell (DAC) and shock wave experiments) and in accurate computational tools. In particular, molecular systems such as hydrogen [2], oxygen [3] and nitrogen [4] have been investigated with a variety of techniques. Nevertheless, fundamental questions on the nature of these systems in e.g. the dense liquid state are yet unanswered.

In this Letter, we focus on the liquid state of oxygen. In particular, we examine the structural and bonding changes induced by pressure, as well as the mechanism leading to the insulator-to-metal transition (ITMT) observed experimentally in shock wave experiments [5].

Metallization of oxygen was first observed in the solid state by Desgreniers *et al.* [6] who reported a Drude-type metallic behavior of its reflectivity for pressures ( $P$ ) above 96 GPa. These results were later confirmed by Shimizu and coworkers [7] who observed a change in the sign of the resistance-temperature curve at 96 GPa, and also discovered superconductivity in solid, dense oxygen [8]. Following measurements by Akahama *et al.* [9], Weck *et al.* [10] showed that in solid oxygen the ITMT is accompanied by a structural change between two different crystallographic arrangements of molecules. The insulating phase below 96 GPa was also studied with infrared absorption spectroscopy by Gorelli *et al.* [11] who suggested the existence of a lattice of  $O_4$  molecules at high pressure. However, this hypothesis is not confirmed by recent *ab initio* calculations [12], showing that a geometrical configuration built from extended “herringbone”-type chains is energetically favored over a lattice of  $O_4$  molecules. The structure predicted theoretically is consistent with earlier suggestions based on DAC experiments [13].

In fluid oxygen, metallization was recently reported by Bastea *et al.* [5] who used reverberation shock wave techniques to generate compression states on a quasi-isentrope. For a given shock speed, the thermodynamic states reached in these experiments are at higher pressure and lower temperatures ( $T$ ) than Hugoniot states obtained in earlier shock wave measurements [14]. When increasing  $P$  from  $\simeq 30$  to 120 GPa (and correspondingly

$T$  by several thousands K), Bastea *et al.* [5] observed an increase of the electrical conductivity over six orders of magnitude. At about 120 GPa and 3.4-fold compression, the measured conductivity attains values characteristic of a poor metal. As  $P$  is further increased from 120 to 190 GPa, the conductivity levels off and is nearly constant as a function of  $P$ . These experimental results, which indicate that the ITMT occurs at higher  $P$  in the liquid than in the solid, are rather surprising. In general, one would expect disorder or dissociation effects to lead to a lower metallization pressure in the fluid than in the ordered solid.

In order to investigate the mechanism by which the ITMT occurs in the fluid, we have carried out a series of *ab initio* molecular dynamics (MD) simulations [15] in the liquid state for different pressures. Our findings shed light on the microscopic structure and electronic properties of the dense fluid state and on the key role of spin fluctuations present in fluid before metallization occurs. Our predicted metallization pressure in the fluid is lower than that reported experimentally [5], as well as lower than the metallization pressure measured in the solid. Our findings further indicate that the system becomes metallic in a predominantly molecular state, as opposed to other fluids like hydrogen [16] and nitrogen [17].

We have carried out *ab initio* MD simulations [15] using a gradient corrected energy functional [18] in the density ( $\rho$ ) and temperature range explored in recent shock wave experiments:  $2.8 \leq \rho \leq 4.5 \text{ g cm}^{-3}$  and  $1000 \leq T \leq 6400 \text{ K}$ . In some of our simulations we have treated the spin variable explicitly within the gradient corrected local spin density approximation (GCSDA). We performed constant volume microcanonical simulations [19] with cells containing 54 and 108 oxygen atoms. For each  $\rho$  and  $T$  the total simulation time was 4–5 ps, after equilibration.

Our calculated pair correlations functions ( $g(r)$ ) are shown in Fig. 1. Finite size effects were found to be negligible compared to temperature and pressure effects. At  $\rho = 2.8 \text{ g cm}^{-3}$  and  $T = 1000 \text{ K}$  [20], the first sharp peak of  $g(r)$  at  $1.20 \text{ \AA}$ , followed by a minimum very close to zero, is indicative of a molecular fluid. The computed pressure is 24 GPa. The first maximum is at a distance very close to the bond length of an oxygen molecule in the

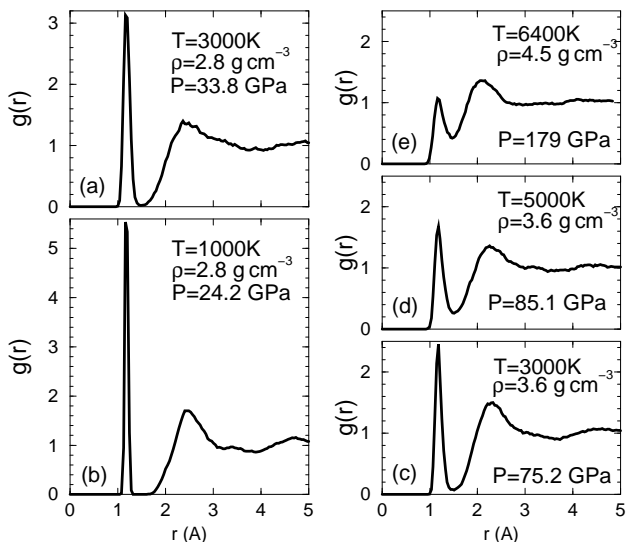


FIG. 1: Pair correlation functions calculated using GCSDA (see text) for different densities, temperatures, and pressures as specified in the legends.

gas phase in its triplet ground state (1.207 Å) [21]. As the temperature is increased to 3000 K (and correspondingly the pressure to 34 GPa) the first molecular peak is broadened while its position remains unchanged. This trend continues as the fluid is compressed to  $\rho = 3.6 \text{ g cm}^{-3}$  at  $T=3000 \text{ K}$  ( $P=84 \text{ GPa}$ ). Upon further compression to  $\rho = 4.5 \text{ g cm}^{-3}$  at  $T=6400 \text{ K}$  ( $P=179 \text{ GPa}$ ), the first molecular peak becomes less intense and the second broad peak moves to shorter distances. It is interesting to note that the position of the intramolecular peak remains constant over a pressure range of 150 GPa and does not shift to larger separations as e.g. in dense liquid hydrogen [22].

The ground state of the  $\text{O}_2$  molecule is a triplet, and this has been shown to give rise to interesting structural effects in the low density fluid [23]. It is therefore interesting to explore the effect of explicit spin treatment on the structural properties of the high pressure fluid as well. We found that spin effects are negligible on average structural properties both at low and high pressure, consistent with recent *ab initio* calculations for solid oxygen [12] in the same pressure range. For example in Fig. 1,  $g(r)$  calculated with and without explicit treatment of spin are found to be indistinguishable. However, spin effects are key in determining the optical excitation spectrum of the low-P fluid, as we will discuss below when we present our results for the electronic conductivity.

The microscopic structure of the liquid can be further examined by a cluster analysis. We define a set of atoms as belonging to a given cluster if these atoms are separated by less than a given cut-off distance  $r_c$ . (We chose  $r_c = 1.50 \text{ Å}$ , which corresponds to the first  $g(r)$  minimum in the molecular regime.) We then define cluster lifetimes by simply computing the duration for which a given clus-

ter remains intact. This analysis yields a very simple picture for our simulations at low density ( $2.8 \text{ g cm}^{-3}$ ) and 1000 and 3000 K: we find that the liquid consists entirely of  $\text{O}_2$  molecules. A density increase to  $3.6 \text{ g cm}^{-3}$  at 3000 K leads to a small fraction of dissociated molecules. Although the liquid is still predominantly molecular (94%  $\text{O}_2$ ), we find 1% single atoms and 5%  $\text{O}_3$ -like clusters. At this density, the average lifetime of  $\text{O}_2$  molecules is about 15 vibrational periods of the isolated  $\text{O}_2$  molecule (21.1 fs), while  $\text{O}_1$  and  $\text{O}_3$  exist only for about one molecular vibration. When the temperature is raised to 5000 K at  $3.6 \text{ g cm}^{-3}$ , the number of molecules decreases to 79%, leading to 7% atoms, 10%  $\text{O}_3$ , and 4%  $\text{O}_4$ -like complexes. The lifetime of molecules decreases to about three  $\text{O}_2$  vibrations, indicating the presence of a dynamical dissociation equilibrium with molecules still being the predominant and most stable species. At  $\rho=4.5 \text{ g cm}^{-3}$  and  $T=6400 \text{ K}$ , we find 9% atoms and 58% molecules and also 16%  $\text{O}_3$  clusters. The remaining 17% of the nuclei belong to short-lived complexes composed of four or more atoms. Further inspection reveals that  $\text{O}_4$ -like clusters arrange predominantly into short zig-zag chains, consistent with the finding of Ref. [12] for the compressed solid. At this high density, the  $\text{O}_2$  lifetime is only about 1.5 vibrational periods. The short lifetime of  $\text{O}_3$  at all densities clearly indicates that triatomic configurations are closer to scattering states than to stable chemical species. Nevertheless, it is interesting to note that the “bond” angles of  $\text{O}_3$  clusters are not randomly distributed but vary between  $80^\circ$  and  $150^\circ$  with an average of  $120^\circ$ . Therefore, the transient structure of  $\text{O}_3$  clusters resembles that of the ozone molecule.

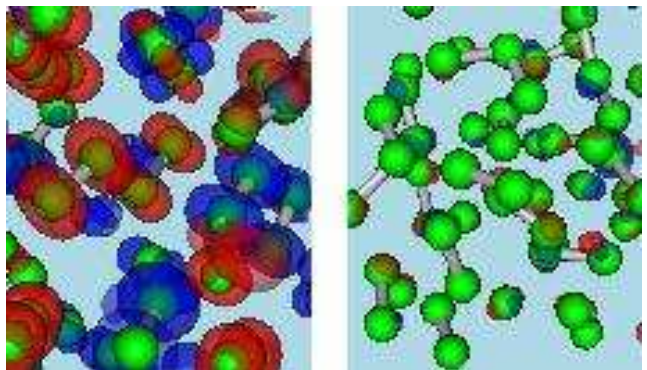


FIG. 2: Difference between spin-up and spin-down densities for two representative snapshots at  $\rho = 2.8 \text{ g cm}^{-3}$  and  $T = 1000 \text{ K}$  (left panel) and  $\rho = 4.5 \text{ g cm}^{-3}$  and  $T = 6400 \text{ K}$  (right panel). Positive and negative regions are represented by red and blue isosurfaces. Green spheres indicate the positions of the atoms.

As mentioned above, while spin effects are negligible for the structural properties of the fluid, it is crucial to include them explicitly in order to understand the electronic properties of liquid oxygen. In the low density

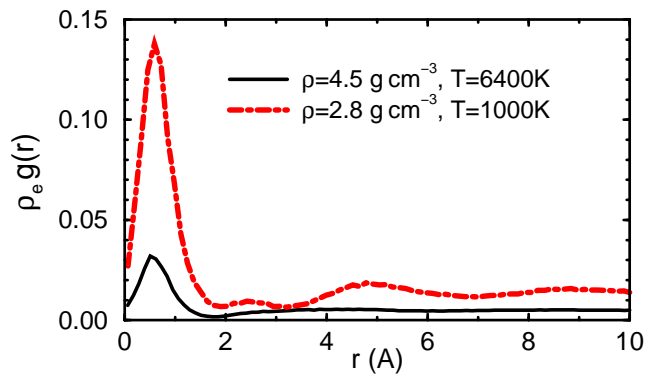


FIG. 3: Pair correlation function derived from nuclear positions and the absolute difference of the spin density. The first peak quantitatively characterizes spin fluctuations present in the molecular liquid at low density of  $2.8 \text{ g cm}^{-3}$ . These fluctuations are suppressed at higher densities.

regime, the liquid is composed of a disordered arrangement of  $\text{O}_2$  molecules carrying a net spin of one as in the gas phase. The left panel of Fig. 2 shows the difference ( $\Delta\rho_{\uparrow\downarrow}$ ) between spin-up ( $\rho_{\uparrow}$ ) and spin-down densities ( $\rho_{\downarrow}$ ), for a snapshot at  $\rho = 2.8 \text{ g cm}^{-3}$  and 1000 K, showing a random distribution of up and down spins. At higher P (right panel of Fig. 2),  $\Delta\rho_{\uparrow\downarrow}$  has almost vanished throughout the whole system, indicating that spin fluctuations are suppressed. The effect shown qualitatively in Fig. 2 can be characterized quantitatively by the correlation function of the nuclei  $\mathbf{r}_i$  and the electronic magnetic moment,  $m_z(\mathbf{r}) = \mu_B[\rho_{\uparrow}(\mathbf{r}) - \rho_{\downarrow}(\mathbf{r})]$ ,

$$\rho_e g_{O,m_z}(|\mathbf{r}|) = \frac{1}{N} \left\langle \sum_{i=1}^N m_z(\mathbf{r}_i - \mathbf{r}) \right\rangle, \quad (1)$$

where  $\rho_e$  is the electron density,  $N$  the number of atoms and  $\langle \dots \rangle$  denotes an average over ionic configurations and the solid angle of  $\mathbf{r}$ . This correlation function is similar to the nuclei-electron pair correlation function. The first, intense peak in the low density correlation function shown in Fig. 3 indicates that the majority of molecules are in the triplet state. At higher density, the intensity of the first peak is decreased by almost an order of magnitude, showing that most of the pairs in the fluid do not carry a net spin.

In order to qualitatively understand the effect of pressure on the spin state of the oxygen molecule, we carried out calculations of the total energies of  $\text{O}_2$  in the singlet ( $E_{S=0}$ ) and triplet ( $E_{S=1}$ ) state in the presence of a confining potential mimicking an average pressure effect. Interestingly, we found that the difference  $E_{S=0} - E_{S=1}$  can be substantially reduced by applying an external confining potential. This difference decreases as a function of the confinement strength.

In order to compare our results with recent shock wave data, we computed the conductivity ( $\sigma$ ) of the liquid for

selected snapshots taken from our GCSDA simulations at different pressures, using the Kubo-Greenwood formula [24, 25]. We note that in the low pressure regime, where spin fluctuations are present, GCSDA and GGA results are very different. In particular, the GGA yields much smaller optical gaps, consistent with the incorrect treatment of excitation in the isolated molecule if spin is not explicitly taken into account. On the other hand, at higher densities, the computed GGA and GCSDA conductivities are very similar.

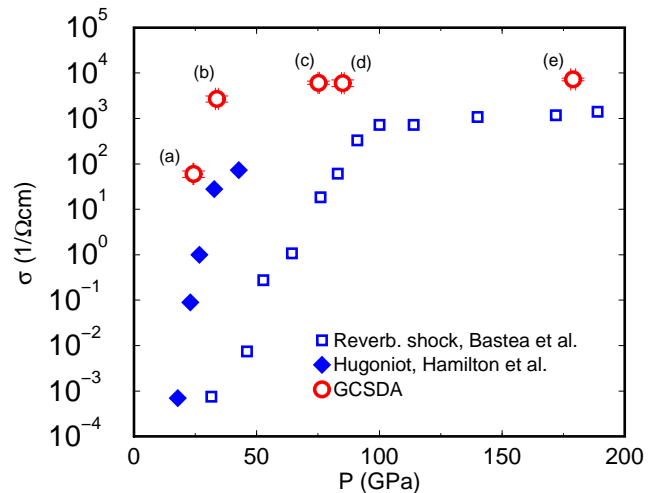


FIG. 4: Measured and calculated conductivity as a function of pressure. The labels on the simulation data points correspond to the thermodynamic conditions specified in Fig. 1.

Our results are reported in Fig. 4 along with the experimental results of Ref. [5] and [14]. The comparison between theory and experiment is not straightforward: the temperature in the measurements by of Hamilton *et al.* [14] is in general different from that of Bastea *et al.*'s data [5], and in both experiments, T was not measured but estimated on the basis of empirical equation of state (EOS) models. However, the two sets of experimental data show the same qualitative rise of  $\sigma$  as a function of P and T. In particular, Bastea *et al.*'s data show a six order of magnitude rise in conductivity with increasing shock compression, corresponding to a P and T increase from about 30 to 120 GPa and 1000 to 5000 K, respectively. Our calculations within GCSDA show only two orders of magnitude increase in  $\sigma$  in the same P and T range. This increase of  $\sigma$  as a function of T occurs primarily in a state where the fluid is entirely composed of stable  $\text{O}_2$  molecules ( $\rho = 2.8 \text{ g cm}^{-3}$ ,  $T = 1000 \rightarrow 3000 \text{ K}$ ). This indicates that in oxygen, metallization is not accompanied by molecular dissociation as found in other first row molecular fluids, in particular hydrogen [25] and nitrogen [17]. Above 100 GPa both theory and experiment show an almost constant  $\sigma$  as a function of compression, but the theoretical values are about a factor of 7 larger than the experimental ones.

In our calculations, overestimates of conductivity values could be due to the use of the GCSDA, which is known to underestimate electronic gaps in many systems. In order to qualitatively investigate this effect, we used a scissors operator and arbitrarily increased the value of the computed gaps by a factor of two. This lowered the computed conductivity by one order of magnitude at  $\rho = 2.8 \text{ g cm}^{-3}$ , both at 1000 and 3000 K. However, even after this “gap correction”, our theoretical data show values of  $\sigma$  approaching those of a poor metal at a pressure much lower (30–40 GPa) than found experimentally. The computed conductivity is then slowly changing as a function of P, and it reaches metallic-like values at approximately 80 GPa. This “slow” metallization of the fluid as a function of pressure may be related to spin fluctuations and their “slow” suppression as a function of pressure. At low P, the molecular fluid, with each oxygen molecule in a triplet state, can be viewed as a disordered spin system. As the pressure is increased, this system shows a glass-like behavior due to the presence of a multitude of local minima in its potential energy surface, corresponding to a multitude of different spin arrangements. Eventually, the fluid reaches metallization when spin fluctuations are almost completely suppressed. In this respect, compressed liquid oxygen is unique among first row molecular fluids and rather different from, e.g. liquid hydrogen and liquid nitrogen, composed of molecules with spin zero.

In summary, our first principles simulations show that above 30 GPa, over a wide pressure range of about 50 GPa, liquid oxygen transforms from a semi-conducting to a metallic fluid by closure of the band gap in a disordered molecular state. For  $P \geq 80$  GPa, molecular dissociation is observed, giving rise to short-lived atomic- and ozone-like species. We did not observe any stable  $\text{O}_4$  molecule for the thermodynamic conditions considered here, which is consistent with recent theoretical findings for solid oxygen [12]. Our results also show that spin fluctuations are suppressed at high pressure, with no significant magnetic moment present in the high pressure liquid, as opposed to the semi-conducting low pressure regime.

Our findings for the electrical conductivity point at the need for further experimental and theoretical work. Experimentally, in shock wave experiments only P and  $\sigma$  are measured. Data are then analyzed using a model EOS as input for hydrodynamic codes which compute densities. Finally, the temperature is inferred from additional empirical chemical model calculations. This type of analysis may introduce uncertainties in the estimated  $\rho$  and T at a given P and  $\sigma$ . Measurements of the oxygen EOS obtained with shock wave experiments and possibly with other techniques, e.g. DAC measurements, may help clarify the existing discrepancies between theory and experiment. Finally, we note that theoretical inaccuracies on calculated conductivity values may arise from the use of an approximate exchange and correlation functional. Although computationally still out of reach,

quantum Monte Carlo calculations for liquid oxygen under pressure might be used in the future to address this issue [16].

We thank M. Bastea for her support of this project and for many useful discussions, D. Young for providing us with EOS tables from chemical models, and L. Benedict, V. Recoules, E. Schwegler, and T. Ogitsu for useful suggestions. This work was performed under the auspices of the U.S. Dept. of Energy at the University of California/LLNL under contract no. W-7405-Eng-48.

- 
- [1] R. J. Hemley. *Annu. Rev. Phys. Chem.* **51**, 763 (2000) and references therein.
  - [2] P. Loubeyre *et al.*, *Nature* **416**, 613 (2002).
  - [3] P. P. Edwards and F. Hensel, *Chem. Phys. Chem.* **3**, 53 (2002).
  - [4] M. L. Eremets *et al.*, *Nature* **411**, 6834 (2001); A. F. Goncharov *et al.*, *Phys. Rev. Lett.* **85**, 1262 (2000).
  - [5] M. Bastea *et al.* *Phys. Rev. Lett.* **86**, 3108 (2001).
  - [6] S. Desgreniers *et al.* *J. Chem. Phys.* **94**, 1117 (1990).
  - [7] K. Shimizu *et al.*, Proceedings of the Adriatico Research Conference: Simple Systems at High Pressures and Temperatures: Theory and Experiment (Abstract no. 15, [http://www.ictp.trieste.it/~pub\\_off/sci-abs/smr999](http://www.ictp.trieste.it/~pub_off/sci-abs/smr999), ICTP, Trieste, October 1997).
  - [8] K. Shimizu *et al.*, *Nature* **393**, 767 (1998).
  - [9] Y. Akahama *et al.*, *Phys. Rev. Lett.* **74**, 4690 (1995).
  - [10] G. Weck *et al.* *Phys. Rev. Lett.* **88**, 035504 (2002).
  - [11] F. A. Gorelli *et al.* *Phys. Rev. Lett.* **83**, 4093 (1999); F. A. Gorelli *et al.* *Phys. Rev. B* **63**, 104110 (2001).
  - [12] J.B. Neaton and N. W. Ashcroft, *Phys. Rev. Lett.* **88**, 205503 (2002).
  - [13] S. F. Agnew *et al.*, *J. Chem. Phys.* **86**, 5239 (1987).
  - [14] D. C. Hamilton, *J. Chem. Phys.* **88**, 5042 (1988).
  - [15] R. Car and M. Parrinello, *Phys. Rev. Lett.* **55**, 2471 (1985).
  - [16] R. Hood and G. Galli, submitted.
  - [17] S. Mazevet *et al.*, *Phys. Rev. B* **67**, 054201 (2003).
  - [18] J. P. Perdew *et al.*, *Phys. Rev. Lett.* **77**, 3865 (1996).
  - [19] All simulations were performed using the parallel *ab-initio* molecular dynamics code, GP version 1.12.0 (F. Gygi, LLNL 1999-2002). We used described the interaction between electrons and ions with a norm conserving pseudopotential [D. Hamann. *Phys. Rev. B* **40**, 2980 (1989)] including angular momenta up to  $l=2$ . The  $l=2$  component was key to obtain accurate properties of the isolated molecule. The calculated  $\text{O}_2$  bond distance is 1.30 and 1.22 Å when including up to  $l=1$  and  $l=2$ , respectively. The experimental bond length is 1.207 Å. We used plane wave basis sets with energy cutoffs up to 95 Ry. 80 Ry was needed to converge structural properties, and 95 Ry for the pressure.
  - [20] This temperature is slightly above the melting temperature of  $\simeq 800$  K obtained by extrapolating the DAC melting measurements by G. Weck (Ph.D. thesis, Université Paris 6, 2001).
  - [21] D. C. Patton *et al.* *Phys. Rev. B* **55**, 7454 (1997).
  - [22] G. Galli *et al.* *Phys. Rev. B* **61**, 909 (2000).
  - [23] T. Oda and A. Pasquarello, *Phys. Rev. Lett.* **89**, 197204 (2002).
  - [24] P. L. Silvestrelli, *Phys. Rev. B* **60**, 16382 (1999).
  - [25] L. A. Collins *et al.* *Phys. Rev. B* **63**, 184110 (2001).